Narrow band UV emission from direct bandgap Si nanoclusters embedded in bulk Si

2010 J. Phys.: Condens. Matter 22 072203

(http://iopscience.iop.org/0953-8984/22/7/072203)

IOP FTC
IOP Publishing
Journal of Physics: Condensed Matter
J. Phys.: Condens. Matter **22** (2010) 072203 (5pp)
doi:10.1088/0953-8984/22/7/072203

FAST TRACK COMMUNICATION

Narrow band UV emission from direct bandgap Si nanoclusters embedded in bulk Si

G Sahu[1], H P Lenka[1], D P Mahapatra[1], B Rout[2] and F D McDaniel[2]

[1] Institute of Physics, Sachivalaya Marg, Bhubaneswar-751005, India
[2] University of North Texas, Denton, TX, USA

E-mail: dpm@iopb.res.in

Received 31 December 2009
Published 2 February 2010
Online at stacks.iop.org/JPhysCM/22/072203

Abstract
We report on the formation of UV emitting Si nanoclusters (NCs) in Si, using a two stage Au implantation technique. These Si NCs, with an average size of 2 nm, show photoluminescence at room temperature, over a narrow band of about 100 meV with a peak of emission near 3.3 eV. With emission lifetimes in the range of 1.5–2.5 ns, the transitions seem to come from excitonic recombinations across a quasi-direct gap. Since the structures are below the surface, there is no adverse effect of oxidation resulting in a shift in emission wavelength. On the other hand, an annealing at 500 °C has been found to result in a significant increase in the emission intensity. This is due to localized plasmon induced electric field enhancement in Au nano-islands in the vicinity.

(Some figures in this article are in colour only in the electronic version)

1. Introduction

The ability of forming Si-based low-dimensional structures, such as quantum-dots, has drawn much attention into the possibility of fabricating nano-optoelectronic devices [1–4]. This is due to the fact that Si nanoclusters (NCs) possess optical and electrical properties quite different from those of bulk Si. For particle sizes below the excitonic Bohr radius ($a_B = 4.3$ nm), Si NCs show a quantum confinement effect [5] resulting in an enhanced recombination of excitons [6]. However, compared to direct bandgap III–V or II–VI semiconductor NCs, the radiative recombination coefficient of Si is rather low at room temperature, $\sim 10^{-14}$ cm^3 s^{-1} [7]. Therefore, even considering the defect mediated recombination and Auger assisted non-radiative transitions to be suppressed due to spatial localization of carriers, in Si NCs, the electron–hole recombination lifetime is rather long, ranging from ms to μs [8]. Despite high internal quantum efficiency, the long recombination lifetime reduces the photon recycling rate even in the absence of a non-radiative process. This results in poor carrier injection efficiencies. The matrix also plays an important role. Bonding to oxygen has been found to result in band mixing with a redshift in the emission wavelength and a suppression of the quantum confinement effect.

Ion implantation is a widely used technique in Si processing involving VLSI applications. This has been used to synthesize Si NCs in SiO_2 through a high fluence implantation of excess Si atoms into the matrix, followed by a thermal annealing [9]. The implantation energy provides a control regarding the depth at which NCs are to be formed, the fluence (no. of atoms cm^{-2}), together with annealing temperature as well as duration, providing a control over their growth. Si NCs synthesized using this method have been found to show photoluminescence (PL) over a rather wide band (1.5–2 eV, width >200 meV) from visible to near infrared region, with a peak of emission around 1.7 eV. The emission has been found to be dominated by defect mediated surface traps. In the present work, we report ultraviolet (UV) emitting Si NC formation, in the near surface region of bulk Si substrates, using a different implantation method. Here a two stage Au implantation is used both for amorphization (at lower energy) and localized recrystallization (at higher energy) of the Si

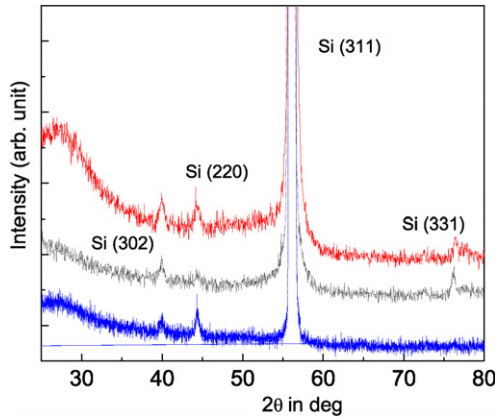

Figure 1. XRD spectra for various samples. The top, middle and bottom spectra are for the Au implanted sample, the Au implanted annealed sample and the Si implanted sample, respectively.

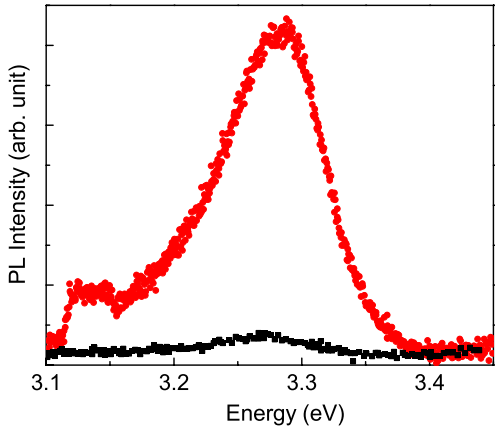

Figure 2. PL spectra for the Au implanted annealed sample (filled circles) and Au implanted unannealed sample (filled squares) recorded at room temperature.

substrate, resulting in NC formation [10]. Since the substrate (bulk Si) has favourable electrical properties as compared to an insulating matrix such as SiO_2, the method is very much suitable for nano-scale device applications. The synthesized NCs show emission with a peak around 3.3 eV, over a narrow band ∼100 meV. Emission lifetimes have been found to be around 2 ns indicating excitonic recombination across a quasi-direct gap. The other advantage of our technique lies in the fact that the NCs are produced below the surface with no fear of oxidation or any other chemical effect which might affect the emission. In addition, due to the presence of Au, an annealing in air has been found to result in an enhanced emission similar to surface enhanced Raman scattering [11].

2. Experiment

In the present study, Si(100) samples (n-type, P doped with resistivity 1–20 Ω cm), were implanted with 45 keV Si^- and 32 keV Au^- ions to fluence of 1×10^{16} and 5×10^{15} ions cm^{-2}, respectively. The implantations were carried out, at room temperature (RT), at beam currents ∼240 nA with a sample tilt of 7° with respect to the surface normal. This was done using a low energy negative ion implantation facility, available at the Institute of Physics, Bhubaneswar (IOPB). The Au implanted Si samples were further implanted with 3 MeV Au^{2+} ions, at RT, to a fluence of 1×10^{15} ions cm^{-2}, using the 3 MV Pelletron accelerator (NEC, USA) facility at IOPB. One of the doubly Au implanted samples was annealed in air at 500 °C for 1 h to look for any possible growth in size of the NCs formed in the matrix. The samples were characterized using x-ray diffraction (XRD), steady state (SS) as well as time resolved (TR) photoluminescence (PL), transmission electron microscopy (TEM) and Fourier transformed infrared (FTIR) absorption measurements. XRD analysis was carried out using Cu Kα radiation at 8.026 keV (Rigaku Altima III). SS PL measurements were carried out at an excitation wavelength of 325 nm using a He–Cd laser (TRIAX 320 spectrometer) while TR-PL measurements were carried out using a mode-locked, frequency doubled, Ti:sapphire laser (pulse width 80 fs, repetition rate 80 MHz) at an excitation wavelength of 350 nm (C4334 Streakscope and Bruker 250IS spectrograph). TEM imaging was carried out at an electron beam energy of 200 keV (FEI G2 F20-ST system). FTIR measurements were carried out using a Thermoelectron Nicolet 6700 system.

3. Results and discussion

First we present the XRD data in figure 1 where the spectra for various samples have been shifted along the y-axis for clarity. As shown earlier [12], the low energy Au implantation to a fluence of 5×10^{15} cm^{-2} is found to amorphize the top 30–40 nm of the Si matrix without any Si NC formation. However, after the second Au implantation at 3 MeV, there is Si NC formation. XRD data as obtained on the doubly Au implanted sample, show the presence of small crystallites. This is evident from the small peaks at 2θ values of 40°, 44.5° and 76.5° corresponding to Si(302), Si(220) and Si(331) reflections. That the system was still largely amorphized can be seen from the broad hump at low angles in the XRD data. The low energy Si implantation resulted in damage production and amorphization over a depth of around 100 nm, the XRD spectrum of which is also included in the figure for comparison. The corresponding spectrum shows reduced amorphization, with small crystallites in the damaged Si lattice. However, unlike the Si implanted case, the Au implanted sample showed PL at RT which confirms NC formation. A further annealing of the Au implanted sample results in a movement of Si NCs and some Au towards the surface. It helps in a partial recrystallization of the amorphized matrix, as seen from the sharpening of the peaks observed in the XRD data. It also results in formation and growth of Au nano-islands embedded in the matrix as well as on the surface.

The SS PL measurements carried out at RT showed Si NC formation in the Au implanted samples. But no signal could be detected at RT for the Si implanted control sample. Figure 2 shows the SS PL spectra of the Au implanted annealed (500 °C, 1 h) and unannealed samples, recorded at RT. It is seen, in both cases, the emission is peaked near 3.3 eV in the UV range. In case of the annealed sample, the emission width (FWHM) of ∼100 meV is almost half of that found in case of Si NCs, prepared in SiO_2 using excess Si implantation [9].

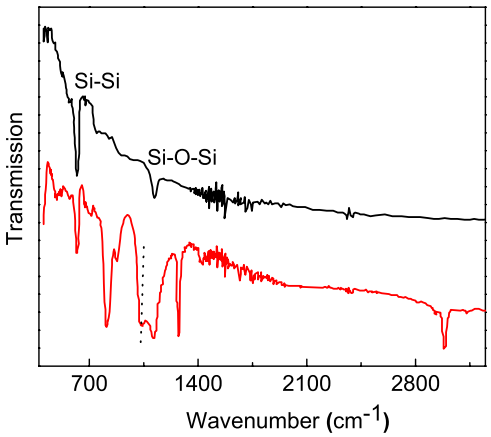

Figure 3. FTIR spectra corresponding to the annealed Au implanted sample (lower) together with that for the Si implanted control sample (upper). The position of the marker on the spectrum for the Au implanted sample corresponds to the surface Si–O–Si stretching vibrations.

The signal for the unannealed sample is seen to be rather weak. However, there is no redshift in the peak position in the case of the annealed sample, as compared to the as-implanted sample. This rules out any growth in size of the NCs effected due to annealing. This also rules out any possible oxidation of the NCs resulting in a size reduction which would have resulted in a blue shift. That the air annealing was not resulting in any oxidation of the Si NCs was confirmed using infrared absorption measurements (FTIR spectroscopy). Results for the Au implanted and annealed sample, together with that for the Si implanted one, are shown in figure 3. No measurable FTIR signal could be obtained from the unannealed Au implanted sample. This is mainly due to scattering of the IR signal in the top amorphized layer dispersed with Au particles. For the Si implanted sample there are strong absorption bands around 613 and 1107 cm^{-1} coming from Si–Si and bulk Si–O–Si vibrational modes [13, 14]. For the annealed Au implanted sample we see an additional band just below the bulk Si–O–Si band, coming from a surface ν(Si–O–Si) stretching mode. Passivation of surface dangling bonds on Si NCs by oxygen is expected to lead to a redshift [14, 15] while an oxidation is expected to result in a size reduction leading to a blue shift, in the PL peak. Since this is not seen, the air annealing is understood to have resulted in a surface oxidation of the bulk Si matrix without affecting the buried NCs. Therefore it appears, the buried Si NC surfaces are already passivated by Au. At low concentrations, ($\sim 10^{15}$ cm^{-2}), Au is known to form a covalent bond with Si [16]. The fluence of Au atoms in the low energy Au implantation (confined to a 30 nm thickness), leads to a Au concentration of the same order. This does not change much since the MeV Au atoms from the second implantation go much deeper (>800 nm). Therefore, the Au concentration, in the top 30 nm of the amorphized region, where Si NCs are formed, does not go too far beyond that for a coverage of about one monolayer, preventing any silicide formation [10, 16].

During annealing a part of the Au atoms diffuse outwards [17, 18] forming islands on the surface. Some also move towards the deeper interface, some passivating the surface of Si NCs formed. This movement of Au has been confirmed through TEM which also shows a lot of Au nano-islands in the matrix. This Au accumulation in the form of NCs has the additional effect of enhancing the electric field in the vicinity of the Si NCs through localized surface plasmon (SP) excitation [19]. During the passage of the laser pulse, there can be localized surface plasmon (SP) excitation in the Au nano-islands. This SP excitation can couple with carrier excitations in Si NPs leading to an enhanced PL signal. This has been seen in case of ZnO nanorods and thin films, coated with Au nano-islands with PL emission in the UV [20, 21]. Such Au SP excitation induced PL enhancement in the visible range has been seen in case of Si NCs embedded in quartz [23]. In the present case bonding of Au atoms and their accumulation on the surface of Si NCs can be imagined to result in the formation of a thin spherical shell of Au. As shown in case of a nearly spherical C_{60} molecule [22], there can be several modes of SP excitations which can play a role regarding electric field enhancement at different frequencies. As will be shown later, in certain cases, there can be enhancement in PL signal in the UV, as observed here.

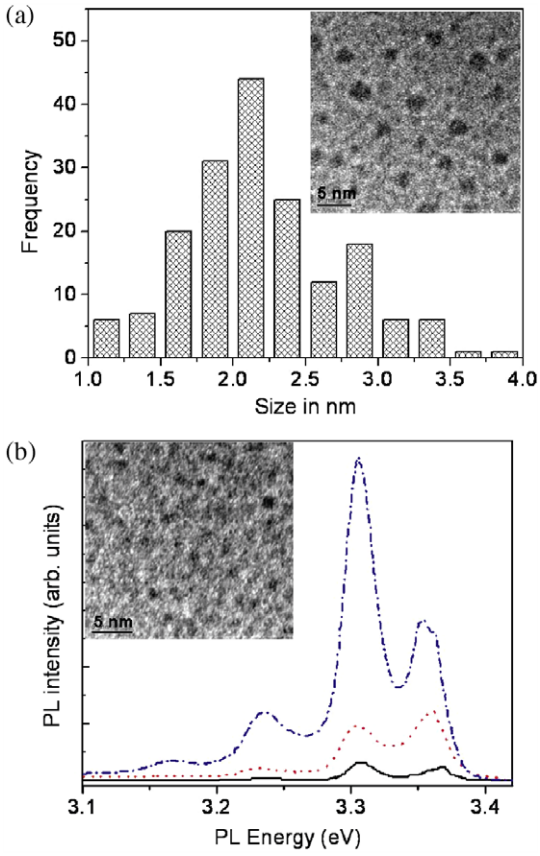

Figure 4. (a) Size distribution of Si NCs formed in the Au implanted and annealed sample. The Inset shows a typical high resolution TEM image. (b) PL spectra recorded at 77 K. The dot-dashed and dotted lines correspond to the Au implanted annealed and unannealed samples respectively. The continuous line correspond to the Si implanted control sample a typical TEM micrograph of which is shown in the inset.

In figure 4(a) we show the size distribution of the Si NCs formed in the Au implanted and annealed sample as

determined from high resolution TEM imaging carried out under diffraction contrast. A typical bright field image corresponding to the region showing PL emission is shown in the inset. The dark contrast in this case comes from crystalline Si NCs sitting in an amorphized Si matrix. To justify this in figure 4(b) we show the PL emission data collected at 77 K on the Au and the Si implanted samples together with a TEM micrograph of the Si implanted control sample. One can see, excepting an enhanced emission in the Au implanted samples, the PL spectra are very similar in all the three cases. The TEM micrographs for the Si implanted case also show features in contrast quite similar to that seen for the Au implanted case. In addition, in the Au implanted samples, we have carried out energy dispersive x-ray (EDX) measurements at the corresponding sites and no measurable signal for Au could be detected. All this indicate that the structures seen in the TEM images are corresponding to Si NCs.

In case of the Au implanted and the annealed sample the average size of Si NCs is seen to be around 2.15 nm. Assuming a bulk energy gap of 1.12 eV together with an infinite potential barrier, the PL emission from Si NCs, at 3.28 eV can be understood in terms of a confinement energy of 9.98 eV nm^2. UV emitting Si NCs have also been synthesized using plasma enhanced chemical vapour deposition technique in Si_3N_4 [1, 2]. Although the confinement parameters are in reasonable agreement with our result the emission widths are larger than that in the present case. Having determined the size of Si NCs, following the work on C_{60} [22], we have estimated the energy of the lowest SP excitation mode for a thin spherical Au shell sitting on a typical Si NC (radius ∼1 nm). For a shell thickness of 0.25 nm (Au–Si covalent bond length), the ratio of the inner to outer radii, α, is about 0.8. In such a case the lowest $l = 1$ mode has an energy of 3.28 eV for an ω_p of 4.75 eV. This corresponds to about 60 electrons coming from an equal number of Au atoms sitting on the Si NC. Typical surface atomic density in Si lies between 6.8 (for 100) and 11.8 (for 111) atoms nm^{-2}. Taking a surface atomic density of 10 atoms nm^{-2} on the Si NCs, 60 Au atoms bonded to the surface would correspond to about 1/2 a monolayer leading to Au passivation. This can result in an enhanced PL intensity compared to no-Au case. The lower intensity as observed for the unannealed Au implanted sample, together with no peak shift, can be understood in terms of a reduced number of surface passivated Si NCs in the matrix.

TR-PL measurements have also been carried out on the Au implanted and annealed sample. For this sample, the emission lifetime, τ, over the entire range of the PL spectrum, (figure 5) is found to vary between 1.5 and 2.5 ns. These data are shown together with a transient PL spectrum recorded with the pulsed laser. The measured values of τ are comparable to those of NCs of direct bandgap semiconductors such as GaN and ZnO. However, there is a systematic drop in τ with increase in energy. In general the radiative recombination rate, $R(=1/\tau)$, is proportional to $E^2 f_{osc}$, f_{osc} being the oscillator strength. Smaller NCs show stronger confinement leading to higher values of R and lower values of τ. This leads to progressively smaller values of τ at higher emission energies as observed. For Si NCs with confinement energy, E_C, ∼1 eV, R of excitons

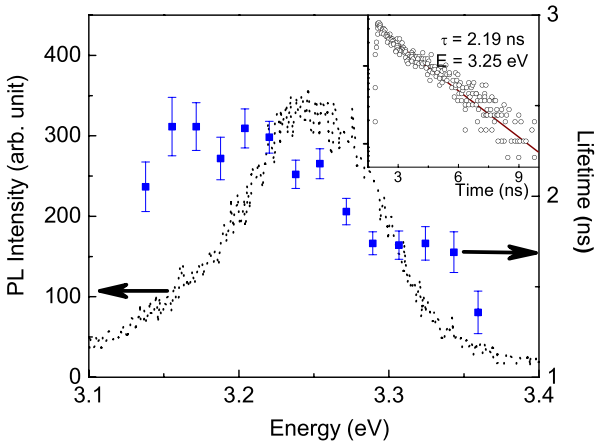

Figure 5. A transient PL spectrum showing emission lifetime, τ, as measured over the entire spectrum for the doubly Au implanted and annealed sample. A typical decay curve corresponding to an energy 3.25 eV, is shown in the inset.

is in the range of 10^2–10^3 ms^{-1} [24]. With an increase in E_C to about 2 eV, as in the present case, R further increases to ∼10^4 ms^{-1} indicating a lifetime ∼100 ns. However, quantum confinement effects result in a mixing of k vectors opening up additional radiative decay channels via zero-phonon pseudo-direct transitions. This happens at $E_C \sim 1$ eV when rates of direct and pseudo-direct recombination are comparable. In smaller NCs with $E_C \sim 2$ eV, R shows an exponential growth due to an increase in strength of pseudo-direct transitions [25]. This is the reason behind getting a very short decay lifetime ∼2 ns which goes in line with quantum confinement effects.

4. Conclusion

In conclusion, we have been able to synthesize Si NCs embedded in Si using a two stage sequential Au implantation technique. The samples, showed luminescence, at room temperature, in the UV, over a narrow emission band ∼100 meV. The emission is consistent with a large confinement parameter ∼10 eV nm^2, indicating good crystallinity. Emission lifetimes have been found to be in the range of 1.5–2.5 ns, indicating transitions corresponding to excitonic recombination across a quasi-direct gap. Improved emission characteristics such as a narrow emission band, very short lifetime for better photon recycling, and an efficient emission in the UV has been obtained which has not been seen earlier.

Acknowledgments

We wish to thank Dr Arup Neogi and his group of University of North Texas (UNT), USA, for their help in carrying out the PL measurements. We acknowledge the help provided by the Centre for Advanced Research and Technology, UNT, regarding sample characterizations. Authors from IOPB also wish to thank Professor S D Mahanti of Michigan State University, USA for some helpful discussions. Authors

from UNT would further like to acknowledge NSF for the IRES grant and support from the UNT Faculty Research and Infrastructure grants.

References

[1] Kim T Y, Park N M, Kim K H, Sung G Y, Ok Y W, Sung T Y and Choi C 2004 *Appl. Phys. Lett.* **85** 5355
[2] Kim T W, Park N, Kim K H and Sung G Y 2006 *Appl. Phys. Lett.* **88** 123102
[3] Lalic N and Linnros J 1999 *J. Lumin.* **80** 263
[4] Choi S H and Elliman R G 1999 *Appl. Phys. Lett.* **75** 968
[5] Wu X L and Xue F S 2004 *Appl. Phys. Lett.* **84** 2808
[6] Lockwood D J 1998 *Ed., Light Emission in Silicon: From Physics to Devices* (San Diego, CA: Academic) chapter 1
[7] Gerlach W, Schlangenotto H and Maeder H 1972 *Phys. Status Solidi* a **13** 277
[8] Hryciw A, Meldrum A, Buchanan K S and White C W 2004 *Nucl. Instrum. Methods Phys. Res.* B **222** 469
[9] Iwayamaa T S, Kurumado N, Hole D E and Townsend P S 1998 *J. Appl. Phys.* **83** 6018
[10] Sahu G, Joseph B, Lenka H P, Kuiri P K, Pradhan A and Mahapatra D P 2007 *Nanotechnology* **18** 495702
[11] Kneipp K, Kniepp H, Itzkan I, Dasari R R and Feld M S 2002 *J. Phys.: Condens. Matter* **14** R597
[12] Christiansen S, Schneider R, Scholz R, Gosele U and Stelzner T 2006 *J. Appl. Phys.* **100** 084323
[13] Tomioka K and Adachi S 2005 *Appl. Phys. Lett.* **87** 251920
[14] Wolkin M V, Jome J, Fauchet P M, Allan G and Deleure C 1999 *Phys. Rev. Lett.* **82** 197
[15] Nishida M 2005 *J. Appl. Phys.* **98** 023705
[16] Iwami M, Tereda T, Tochihara H, Kubota M and Murata Y 1998 *Surf. Sci.* **194** 115
[17] Stelzner Th, Andre G, Wendler E, Wesch W, Scholz R, Gosele U and Christiansen S 2006 *Nanotechnology* **17** 2985
[18] Mohapatra S and Mahapatra D P 2004 *Nucl. Instrum. Methods* B **222** 49
[19] Lee J, Govorov A O, Dulka J and Kotov N A 2004 *Nano Lett.* **4** 2323
[20] Zhang Y, Li X and Ren X 2009 *Opt. Express* **17** 8735
[21] Lin H Y, Cheng C L, Chou Y Y, Huang L L and Chen Y F 2006 *Opt. Express* **14** 2372
[22] Michalewicz M T and Das M P 1992 *Solid State Commun.* **84** 1121
[23] Biteen J S, Pacifici D, Lewis N S and Atwater H A 2005 *Nano Lett.* **5** 1768
[24] Delerue C, Allan G and Lannoo M 1993 *Phys. Rev.* B **48** R11024
[25] Sykora M, Manogolini L, Schaller R D, Kortshagen U, Jurbergs D and Klimov V I 2008 *Phys. Rev. Lett.* **100** 067401